iScience

CellPress
OPEN ACCESS

Article

System concentration shift as a regulator of transcription-translation system within liposomes

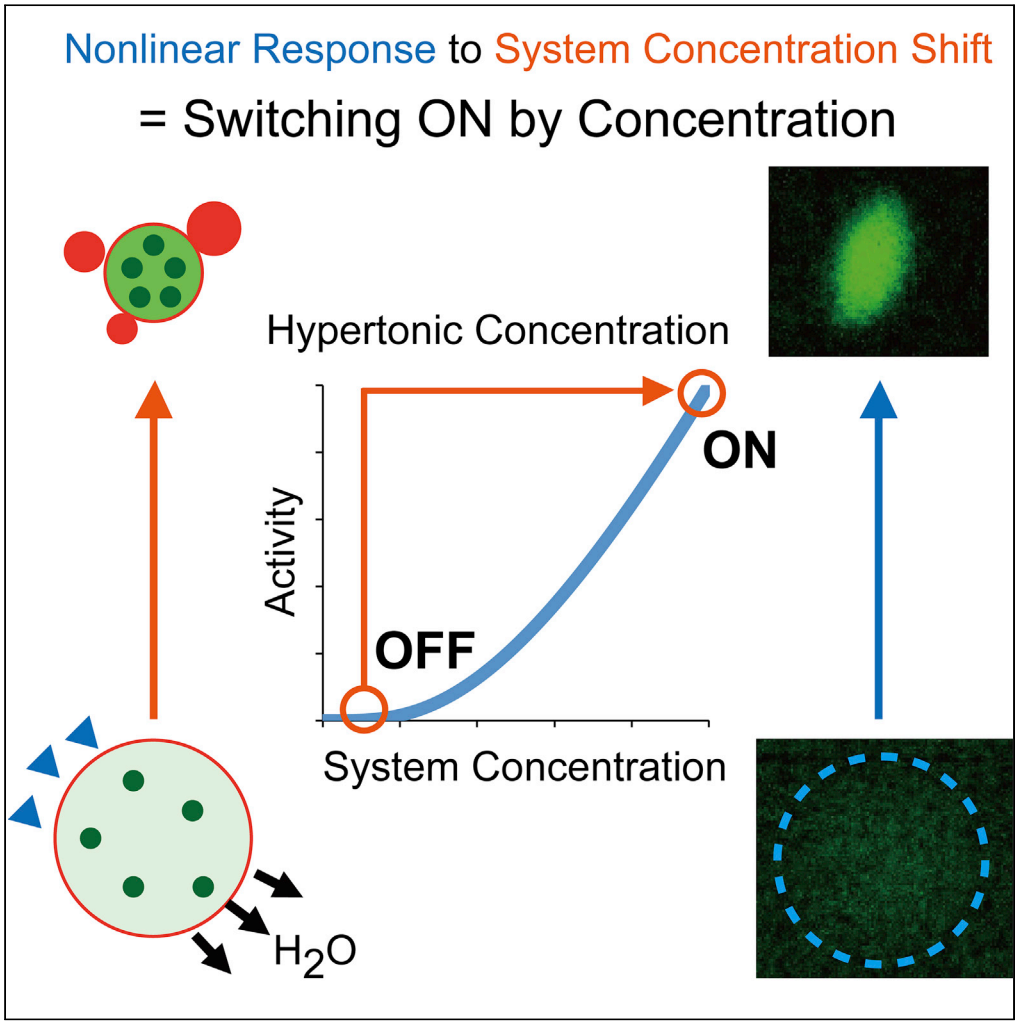

Toshiki Akui, Kei Fujiwara, Gaku Sato, Masahiro Takinoue, Shin-ichiro M. Nomura, Nobuhide Doi

fujiwara@bio.keio.ac.jp

Highlights

Activity of TX-TL changes nonlinearly to the system concentration

By using the nonlinearity, switching of TX-TL in artificial cells was demonstrated

The switching system conferred molecule transfer ability to the artificial cells

The findings provide insight into protocell studies and molecular robotics

Akui et al., iScience *24*, 102859
August 20, 2021
https://doi.org/10.1016/j.isci.2021.102859

iScience

CellPress
OPEN ACCESS

Article

System concentration shift as a regulator of transcription-translation system within liposomes

Toshiki Akui,[1,4] Kei Fujiwara,[1,4,5,*] Gaku Sato,[1] Masahiro Takinoue,[2] Shin-ichiro M. Nomura,[3] and Nobuhide Doi[1]

SUMMARY

Biochemical systems in living cells have their optimum concentration ratio among each constituent element to maintain their functionality. However, in the case of the biochemical system with complex interactions and feedbacks among elements, their activity as a system greatly changes by the concentration shift of the entire system irrespective of the concentration ratio among elements. In this study, by using a transcription-translation (TX-TL) system as the subject, we illustrate the principle of the nonlinear relationship between the system concentration and the activity of the system. Our experiment and simulation showed that shifts of the system concentration of TX-TL by dilution and concentration works as a switch of activity and demonstrated its ability to induce a biochemical system to confer the permeability of small molecules to liposomes. These results contribute to the creation of artificial cells with the switch and provide an insight into the emergence of protocells.

INTRODUCTION

Biochemical systems such as transcription-translation (TX-TL), glycolysis, and DNA replication consist of various elements and have functions under various interaction and cooperation among the elements. For example, the TX-TL system proceeds by a continuous association and dissociation between DNA and RNA polymerase, between mRNA and ribosome, and between ribosome and aminoacyl-tRNA, and so on (Shimizu et al., 2001; Ramakrishnan, 2002; Murakami and Darst, 2003; Browning and Busby, 2004; Hahn, 2004). In the case of glycolysis, various feedback mechanisms regulate its system activity by sensing the metabolic level, and the concentration of the intermediate metabolite fluctuates under a certain condition (Millard et al., 2017). It has also been known that DNA replication has complicated regulatory dynamics to control the timing and frequency of genome replication (Mott and Berger, 2007; Parker et al., 2017). In a biological system in which such various control mechanisms exist, a dynamic response does not always proceed as expected because the biological system exhibits a nonlinear response to an external signal or a change in the concentration of each element.

As an interesting point in the nonlinear response, dilution or concentration of the whole system can shift behaviors or activities of the systems. Namely, the system dynamics changes nonlinearly even when the concentration ratio of the system components is maintained (hereafter we call this whole dilution or concentration of all system elements as system concentration shift). For example, Min waves, which determine cell division plane of bacteria, change their dynamics modes of spatiotemporal patterning by the system concentration shift among no wave, wave propagation, and heterologous localization on membranes (Kohyama et al., 2019, 2020; Yoshida et al., 2019). As another example, a simplified ethanol synthesis pathway by using three enzymes with the recycling of coenzymes shows a nonlinear behavior of the synthesis rate with respect to the system concentration shift (Fujiwara et al., 2018). It has been also known that even a simple single-molecule catalytic enzyme that degrades polymers behave nonlinearly with respect to the enzyme concentration (Matsuno et al., 1978). Therefore, the system concentration is a factor that regulates the system dynamics.

The importance of system concentration suggests an insight into protocell studies. At the stage of protocells, concentrations of systems are estimated to be lower than those in present living cells (Pereira de Souza et al., 2011) in which macromolecular concentration reaches 100–300 mg/mL(Zimmerman and Trach,

[1]Department of Biosciences & Informatics, Keio University, Yokohama 223–8522, Japan

[2]Department of Computer Science, Tokyo Institute of Technology, Yokohama, Kanagawa 226-8502, Japan

[3]Department of Robotics, Graduate School of Engineering, Tohoku University, Sendai 980-8579, Japan

[4]These authors contributed equally

[5]Lead contact

*Correspondence: fujiwara@bio.keio.ac.jp

https://doi.org/10.1016/j.isci.2021.102859

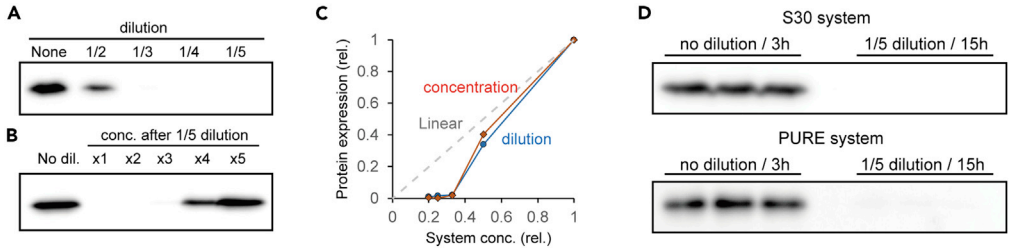

Figure 1. The relationship between TX-TL activity and its system concentration

(A) sfGFP expression levels when the TX-TL system using cell extract (S30) was diluted with ultrapure water (from one-fifth to half). None indicates a no dilution reaction.

(B) sfGFP expression levels of the one-fifth-diluted TX-TL system after being concentrated by evaporating water under argon gas. (A and B) The levels of sfGFP expression after 3 h reaction at 37°C was shown by non-boiling SDS-PAGE.

(C) Relationship between the system concentration and sfGFP synthesis levels at dilution and concentration. The red and blue lines indicate the cases of dilution and concentration, respectively. The gray dotted line indicates the case where the protein synthesis levels show a linear decrease with the dilution of the system concentration.

(A–C) A representative result was shown. All experiments were checked for reproducibility in the experiments carried out on another day.

(D) sfGFP expression levels after extension of reaction times to correspond to the dilution rate. TX-TL was performed using the S30 system or PURE system with dilution or not for 15 h in the case of the dilution sample and for 3 h in the case of the no dilution sample at 37°C. Each lane shows triplicate of the experiments.

1991; van den Berg et al., 2017). Therefore, the TX-TL system, a fundamental system for living cells, must work under such diluted environments. However, recent studies have shown that a dilution of the TX-TL system greatly reduces the TX-TL activity (Fujiwara and Nomura, 2013; Stano et al., 2013; Fujiwara et al., 2014). To understand the possible situation in which protocells emerged, it should be elucidated how the activity of the TX-TL system changes with respect to the system concentration shift.

In this study, we analyzed the changes in protein expression activity of TX-TL systems using cell extracts and the PURE system against the system concentration shift. Experiments and simple simulations targeting the changes of protein expression levels by dilution or concentration showed that TX-TL activity showed nonlinear traits by the system concentration shift. By applying the finding, we successfully achieved the switching of TX-TL activity within the artificial cells from OFF to ON triggered by the system concentration shift. The switching of TX-TL activity within the artificial cell resulted in the spontaneous exchange of small molecules with the outside via expressed membrane proteins. These results demonstrate that the system concentration shift by environmental changes like drying or osmotic pressure can trigger the emergence of biochemical systems. Furthermore, the method provides a new methodology to create artificial cells that can change internal biochemical activity by sensing environments as molecular robots, contributing to bottom-up synthetic biology and biotechnological developments.

RESULTS

Protein expression activity of the TX-TL system changes in a nonlinear manner with the system concentrations shifts

Previous studies have shown that dilution of the system concentration decreases the activity of protein expression by the TX-TL system (Fujiwara and Nomura, 2013; Stano et al., 2013; Fujiwara et al., 2014). However, it was still elusive how the activity of the TX-TL system changes with respect to the system concentration shift. Thus, we investigated the relation between the TX-TL activity and the system concentration. If the relationship is linear, dilution decreases the TX-TL activity linearly. By contrast, if the relationship is nonlinear, dilution greatly decreases the protein expression levels like a switch. Switch in this study indicates the transition of the states of biochemical systems from the levels lower than detection limits (OFF) to detectable and sufficient levels for the functionality of the system (ON). To clarify the point, the concentration of the TX-TL system using cell extract was diluted with ultrapure water, and the relationship between the dilution rate and the amount of protein synthesis was verified. TX-TL activity was evaluated by the levels of sfGFP expression. Consequently, the dilution greatly decreased protein expression levels like a switch (Figure 1A).

The above results indicated that TX-TL activity changes nonlinearly to the system concentration shift. However, one can suppose that the dilution itself induces aggregation or dysfunction of components in

the TX-TL system, which can also explain nonlinear decrease of protein expression levels. To check this point, the diluted system was also concentrated by evaporation under argon gas. The experiments showed that the concentration by the evaporation restores the protein expression activity of the diluted system (Figures 1B and S1A). In both cases of dilution and concentration, the relationship between the system concentration and the amount of protein synthesis showed a very high correlation ($r > 0.99$) (Figure 1C).

The non-linearity of TX-TL activity against the system concentration shift was also confirmed by extending the reaction time. If the relationship is linear, the extension of the reaction time compensates for the decrease of TX-TL activity. We compared the GFP expression levels of 3-h reaction using no dilution TX-TL system with that of 15-h reaction using 5-fold dilution TX-TL system. In any case of TX-TL using cell extract (S30) or purified enzymes (PURE system), the extension of protein expression times did not compensate for the decrease of the protein expression levels (Figure 1D). These experimental results showed that the TX-TL activity behaves in a nonlinear manner with the changes of the system concentration shift.

Analysis of the relation between TX-TL activity and the system concentration shift by a biochemical simulation using a coarse-grained model

To clarify the relation between the TX-TL activity and the system concentration shift, we evaluated the relation by a biochemical simulation using a simple TX-TL model proposed in a previous study (Mavelli et al., 2015). This model extensively simplifies the TX-TL reactions. Transcription is expressed as one-step RNA generation by interaction of DNA and NTP, and translation is expressed as aminoacylation of tRNA by NTP and amino acids, protein synthesis by NTP and the aminoacyl tRNA, and the release of free tRNA (Figure 2A). RNA and proteins behave like a single particle, and they are degraded at a certain rate. The energy regeneration process to convert NXP to NTP is expressed by the system using creatine phosphate and creatine kinase (CP-CK). The simulation using this simple model showed that the relationship between TX-TL activity and the system concentration shift was clearly nonlinear as shown in the experiment (Figure 2B). Similar nonlinearity was also found in a previous study using the same model (Mavelli and Stano, 2015).

Next, concentrations of several components were fixed while those of the others were varied, and the relationships between TX-TL activity and the concentration shift were investigated. Concentrations of small molecules (NTP, CP, amino acids) were fixed, and initial concentrations of macromolecules were varied (Figure 2C,2D). First, we fixed the DNA concentration and varied the concentrations of the other macromolecules and found that DNA dilution only does not affect the nonlinear relationship (Figure 2C, green line). The simulation result was reproduced by a wet experiment using various concentrations of the cell extract (Figure S1B). Second, concentrations of TX elements (DNA and RNA polymerase) were fixed and concentrations of the others were varied. In this case, the relationship between protein levels and concentration shifts became linear (Figure 2C, red line). Third, TX levels were varied, and the others for TL were fixed. In this case, a nonlinear relationship was found, but the relation became near linear and a large decrease during the concentration shift was diminished (Figure 2C, orange line). The sigmoidal-like response to the system dilution is due to abundance of DNA and TX molecule, and the decrease of initial concentration of DNA and TX molecule changed the response pattern (Figure S2A).

To investigate the dependence of each sub-system in TX-TL on system concentration, we simulated a TL-only reaction model in which TX processes were omitted from the simulation model and RNA was supplied as a component (Figure 2D, blue line). In this case, the concentration shift of the entire system components showed the nonlinear relationship. However, in the case in which RNA concentration was fixed and concentrations of other macromolecules were varied, TL activity decreased linearly to the concentration shifts (Figure 2D, red line), similarly to the TX-TL model with fixed TL. To clarify the mechanism behind nonlinearity of the dilution response of TX-TL, we simulated TL reaction by PURE system simulator (Matsuura et al., 2017), which implements all reactions associated with TL reaction. The detailed simulation supports that both RNA and TL elements dilutions are critical for the nonlinear response to the dilution of system concentration (Figure S2B). These results indicated that the concentration shift of both RNA and the translation machinery is necessary for the nonlinear relationship with protein synthesis levels. A plausible explanation is that the nonlinearity is derived from second-order reactions based on the association of RNA and TL systems. Therefore, we concluded that the interaction process between RNA and the translation machinery is the factor of the nonlinear relationship between TX-TL activity and the system concentration shift.

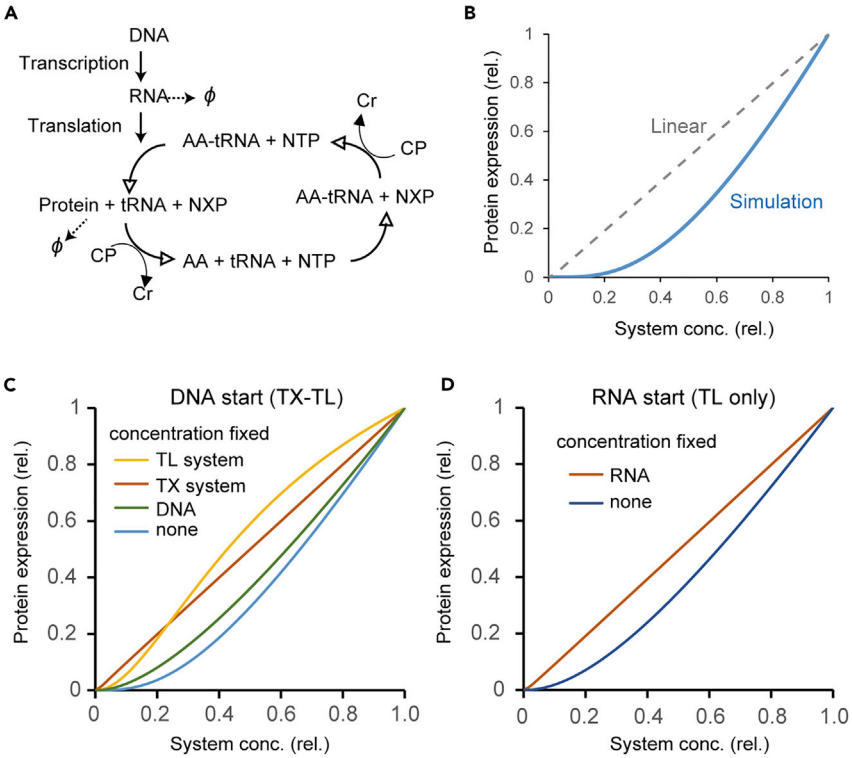

Figure 2. Relationship between system concentration and protein synthesis level in a simplified transcription-translation simulation

(A) Summary of the biochemical model simulated in this study. AA, CP, Cr, and ϕ indicate amino acids, creatine phosphate, creatine kinase, and degradation, respectively.

(B) The relationship between the system concentrations including small molecules and protein expression levels. The gray dotted line indicates the case of linear relation.

(B and C) Protein expression levels are normalized by the case of parameters used in the previous study (Mavelli et al., 2015).

(C and D) The relationship between the system concentrations of macromolecules and protein expression levels. Simulation results of TX-TL reactions (C) and TL only reactions (D) with various system concentrations are shown. Elements without dilution (fixed concentration) are indicated. Concentrations of small molecules are fixed in both simulations.

Switching ON of TX-TL activity of a diluted system by the system concentration shift inside liposome induced by osmotic pressure

The non-linear relationship between the system concentration of the TX-TL system and protein expression levels shown above indicates that TX-TL activity is remarkably low in the case of low macromolecule concentration. This property is unfavorable for protocells in which the concentration of macromolecules is low because spontaneous synthesis of functional proteins is supposed to be a rare event at the time. Therefore, an event to increase the concentration of macromolecules in the TX-TL system should have happened for the functionality of protocells. There are various possible mechanisms for increasing the element concentration such as drying (Mulkidjanian et al., 2012) and synthesis of macromolecules within cell membranes (Mansy et al., 2008). However, drying and synthesis do not essentially ensure a simultaneous increase in all components of the system. By contrast, hypertonic concentration, which raises the concentration of macromolecules entrapped inside liposomes, simultaneously increases all components of the system, because all elements exist in the same space in advance.

Lipid bilayers as the membrane of liposomes are semipermeable, and the internal volume of liposomes changes depending on the osmotic pressure difference between the inside and outside of liposomes. By hypertonic concentration, molecules that remain within the lipid membrane, such as macromolecules and polar molecules, are concentrated when the external osmotic pressure is high. We tested the hypertonic concentration to concentrate 100 μg/mL GFP entrapped within liposomes and found the internal components can be concentrated up to 30 times (~3 mg/mL) (Video S1, Figures S3A and S3C).

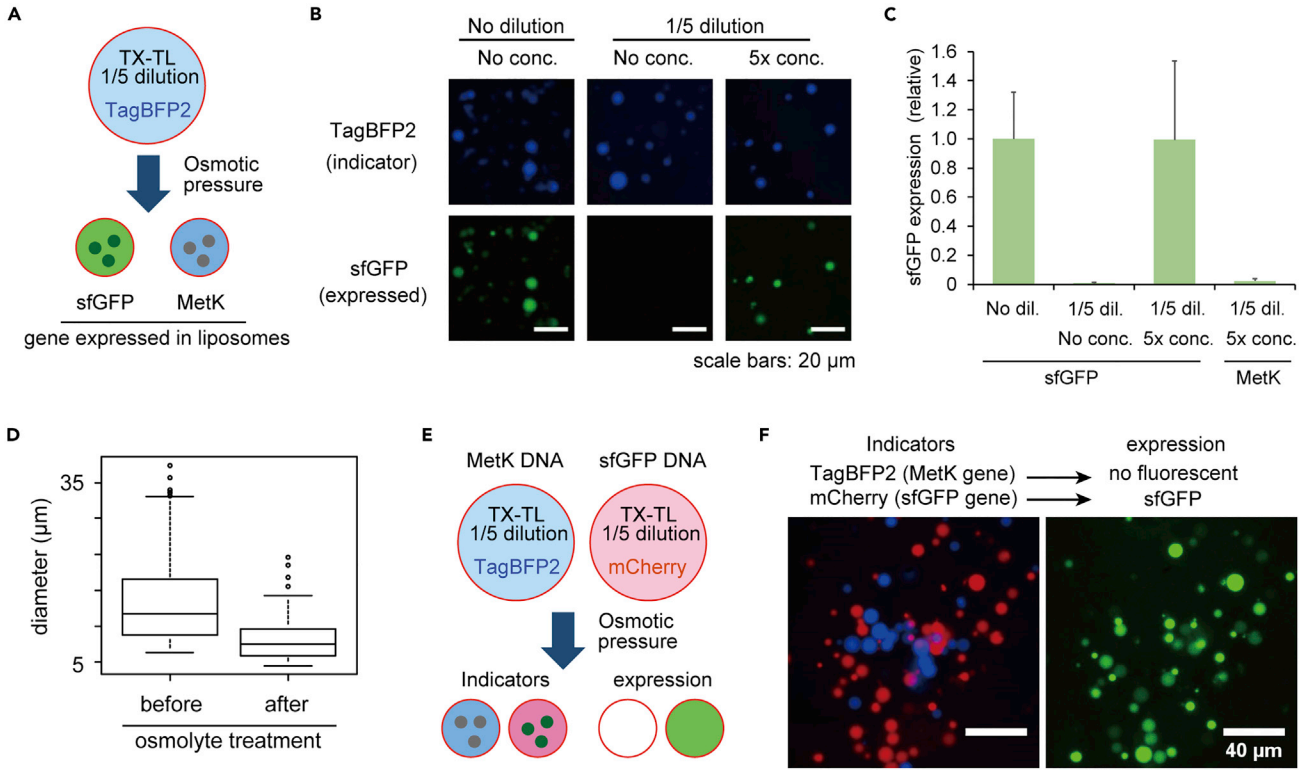

Figure 3. Activation of a diluted TX-TL system within liposomes by hypertonic concentration

(A) Representative illustration of the experiments. In addition to the one-fifth diluted TX-TL system, TagBFP2 protein was added as an indicator of liposomes. Liposomes with GFP expression show both blue and green fluorescence, and liposomes with no GFP expression show only blue fluorescence.

(B) Fluorescence images (non-confocal microscopy) of liposomes encapsulating TX-TL with normal concentration or with one-fifth -dilution. 5x conc. indicates the liposomes after hypertonic treatment. Liposomes were incubated at 37°C for 3 h to express protein.

(C) sfGFP expression levels estimated by confocal microscopy. The levels of sfGFP expression were normalized by the average expression levels of liposomes entrapping normal concentration of the TX-TL system (No dil.). Data are represented as mean ± SD (n = 27, 19, 7, 16).

(D) Boxplots of diameter of liposomes after the hypertonic concentration (n = 134 for before, n = 79 for after the treatment).

(E and F) Simultaneous analysis using bicolor liposomes. The liposome with MetK DNA was marked with TagBFP2 protein, and the liposome with sfGFP DNA was marked with mCherry protein. Representative illustration of the experiments (E) and the results (F). Scale bars: (C) 20 μm and (D) 40 μm.

To verify whether the hypertonic concentration can switch the TX-TL activity, we prepared liposomes entrapping a one-fifth diluted cell extract system for TX-TL using sfGFP DNA as a template and TagBFP protein as an indicator of liposomes (Figure 3A). As a negative control, liposomes entrapping metK DNA instead of sfGFP DNA were also prepared (Figure 3A). However, hypertonic treatment using sucrose used in previous studies induced no observable GFP expression in each liposome. We assumed the dysfunction of the TX-TL system is due to leakage of small molecules for protein expression, and therefore, the mixture of small molecules for TX-TL was used for the hypertonic treatment. In this case, obvious green fluorescence was found in liposomes with sfGFP DNA (Figure 3B), and quantitative analysis by a confocal microscope supported the result (Figure 3C). We also tested the PURE system instead of the cell extract system and found that the hypertonic concentration induced GFP expression inside liposomes in a one-fifth diluted PURE system (Figure S3DE). The diameters of liposomes decreased by 33% after the hypertonic treatment, which matched the expected diameter shift when the volume of liposome decreases one-fifth before the treatment (Figure 3D).

To remove the possibility of artifacts during liposome processing, we prepared two types of liposomes: one containing TagBFP2 protein with MetK DNA and the other containing mCherry protein with sfGFP DNA, and these two types of liposomes were mixed and molecules inside the liposomes were simultaneously concentrated by hypertonic treatment (Figure 3E). Analysis of the fluorescent levels after binary processing after 37°C incubation for protein expression indicated that at least 72% mCherry liposomes and no TagBFP2 liposome showed the green fluorescence, respectively (Figures 3F and S3F). These results clearly show that the hypertonic concentration actually induced switching ON of a diluted TX-TL within liposomes.

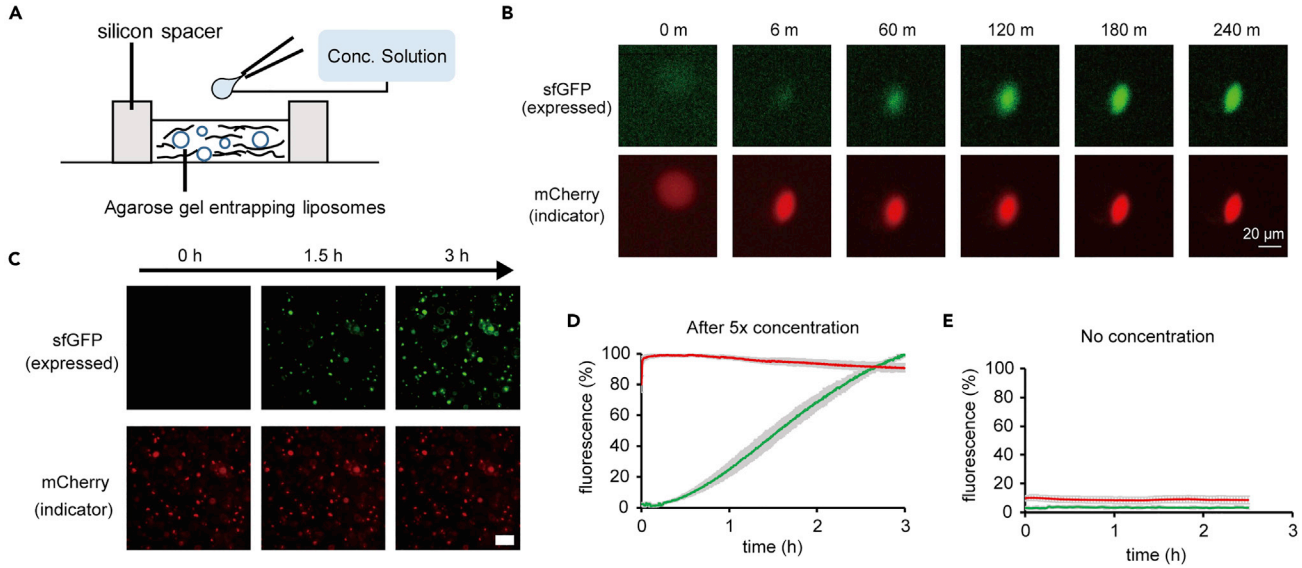

Figure 4. Analysis of time dependence of TX-TL activation by hypertonic concentration with internal macromolecular concentration shift

(A:) A representative illustration of hypertonic concentration of liposomes immobilized by agarose gel. The mixture of liposomes with agarose were gelled in the space prepared by a silicon spacer.

(B) A representative fluorescent image of liposomes after hypertonic treatment. The scale bar indicates 20 μm.

(C) Overview of fluorescent images of sfGFP expressed and mCherry as an indicator of system concentration at 0, 1.5, and 3 h after hypertonic concentration. The scale bar indicates 100 μm.

(D and E) Time plots of fluorescent intensities of sfGFP (green line) and mCherry (red line). Averages of the results from four independent experiments with (D) and without (E) hypertonic concentration are shown by green and red lines. Gray areas indicate standard deviation from four independent experiments. The y axis shows fluorescence intensities normalized by the maximum value in D and does not directly show the concentration of molecules. All experiments were checked for reproducibility in another day experiment. The maximum fluorescence intensity of sfGFP and mCherry after hypertonic concentration was set at 100%.

Time response of activation of a diluted TX-TL system within liposomes by hypertonic concentration

Next, we analyzed the time response of the activation of a diluted TX-TL system within liposomes by hypertonic concentration. For the long-time imaging of the same liposomes, the movement of the liposomes due to Brownian motion should be prevented. Thus, we immobilized liposomes by entrapping them in agarose gel (Figure 4A). In this experiment, fluorescence of sfGFP expressed by the activated TX-TL and the fluorescence of mCherry were used as an indicator of internal macromolecular concentration shifts within liposomes. After hypertonic concentration, mCherry fluorescence increased rapidly (Figure 4B, Video S2). The shape of liposomes became crescent rather than spherical after hypertonic concentration owing to the immobilization inside the gel (Figure 4B, Video S2). After the increase of mCherry fluorescence, sfGFP fluorescence increased gradually with time up to 3 h (Figure 4C, 4D, Video S2, S3). Such an increase in mCherry concentration and synthesis of sfGFP were not observed without hypertonic concentration (Figure 4E). The time-dependent increase of sfGFP synthesis after hypertonic concentration was similar to that observed in *in vitro* expression or in liposome expression using a normal concentration of the TX-TL system, suggesting that the hypertonic concentration activates a diluted TX-TL to the normal level.

Transport of small molecules by expression of a membrane protein utilizing system concentration shift via hypertonic concentration

Membrane proteins that enable exchange of small molecules with the outside are required for the sustainable functionality of TX-TL systems. Thus, we tested if hypertonic concentration can express a small molecule transporter, α-hemolysin (α-HL), which is widely used in synthetic biology and has a pore that does not have substrate specificity (Noireaux and Libchaber, 2004; Wu and Tan, 2014; Fujii et al., 2013; Hilburger et al., 2019; Buddingh et al., 2020). Similar to the case of sfGFP expression, we prepared liposomes containing either α-HL gene or *metK* gene (Figure 5A). In addition to the diluted TX-TL system, each liposome contained calcein, which is impermeable without the pore of α-HL owing to its relatively larger molecular size

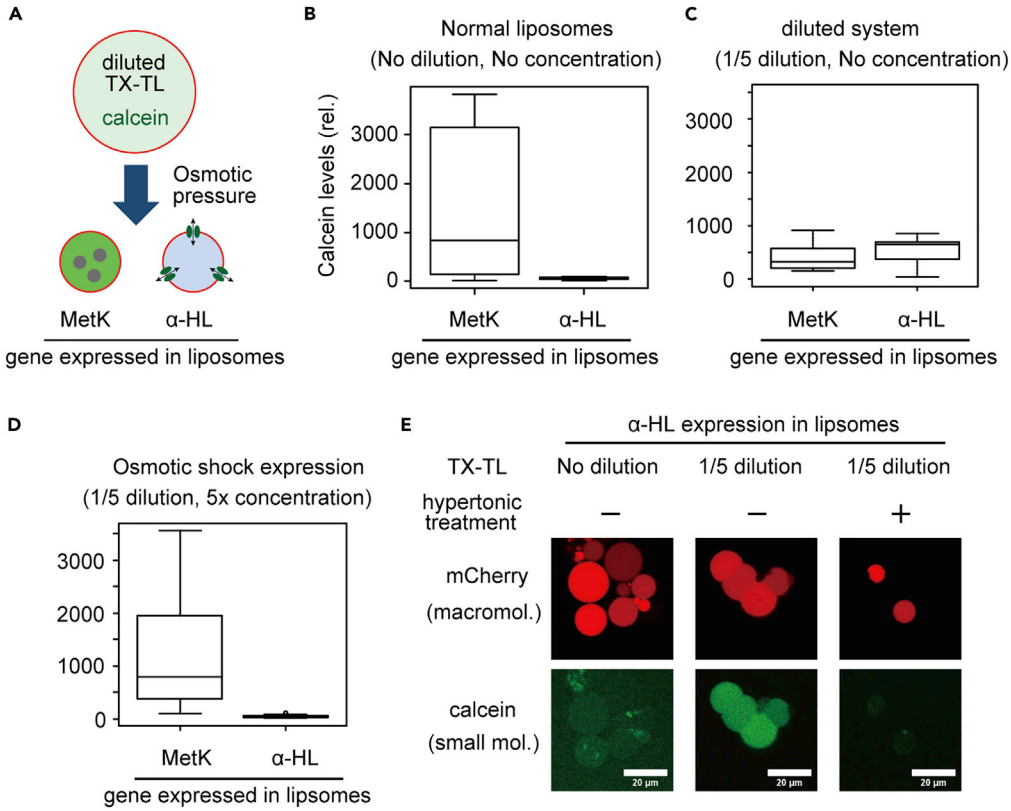

Figure 5. Transportation of small molecules through membrane protein synthesis by activation of the TX-TL system via hypertonic concentration

(A) A representative illustration of the experiment. Liposomes contain one-fifth-diluted TX-TL system, mCherry protein, and either α-HL or MetK DNA. In the case of MetK expression, calcein stays inside the liposomes, and in the case of α-HL expression, calcein leaks out from the liposomes.

(B–D) Fluorescence intensities of calcein. (B–D) Boxplots of the calcein levels in liposomes after TX-TL reaction. (B) Liposomes contain a TX-TL system of normal concentration with MetK DNA (n = 22) or α-HL DNA (n = 47). (C) Liposomes contain one-fifth-diluted TX-TL system with MetK DNA (n = 11) or α-HL DNA (n = 8). Calcein levels are lower than the normal or 5x concentration cases because of its concomitant dilution during the dilution process. (D) Liposomes contain one-fifth-diluted TX-TL system with MetK DNA (n = 27) or α-HL DNA (n = 17) in the case of hypertonic concentration.

(E) Fluorescent images of mCherry (macromolecule) and calcein (small molecule) within liposomes after α-HL expression shown in Figures 5B–5D. Qualitative reproducibility of these results was confirmed in an experiment performed another day. Scale bars indicate 20 μm.

and electric charge. As a control, a macromolecule that is impermeable regardless of α-HL, mCherry protein, was also entrapped in the liposomes. In liposomes with the TX-TL system of normal concentration, calcein disappeared owing to α-HL expression in contrast to liposomes with MetK expression (Figure 5B). On the other hand, in the liposome encapsulating the diluted TX-TL system, no clear difference of calcein signals was observed between α-HL and MetK liposomes (Figure 5C), which supports impermeability of calcein under hypertonic treatment. Of the liposomes encapsulating the diluted TX-TL system with hypertonic concentration, α-HL liposomes showed complete leakage of calcein but kept mCherry, similarly to the α-HL liposome with TX-TL system of normal concentration (Figure 5D, 5E and S4). These results demonstrate that the activation of the TX-TL system inside liposomes by the increase of its system concentration via hypertonic concentration can develop a system to transport small molecules through cell membranes.

DISCUSSION

In this study, we showed that the concentration of all the constituent elements (system concentration) is an important factor to determine the protein expression levels of the TX-TL system. The results indicate that rapid increase of macromolecular concentration behaves like a switch of the system from OFF to ON.

Because there are many biochemical systems whose activities and behaviors changes non-linearly by the system concentration shift, it is possible that switching by the system concentration shift plays an important role in biochemical systems.

The switching character of the TX-TL system suggests the importance of macromolecular concentration shift for the emergence of protocells. Before the emergence of primitive life, it is assumed that macromolecules were not abundant in the environment. Therefore, several possible mechanisms that could have concentrated macromolecules inside liposomes have been proposed. Although it was proposed for concentration of ions, drying by evaporation on thermal field is a plausible mechanism (Mulkidjanian et al., 2012). Another report showed that synthesis of macromolecules by charged small molecules that go through membranes may have caused the increase of macromolecular concentration within liposomes (Mansy et al., 2008). There are studies that pointed out a possibility that overcrowding of macromolecules during liposome formation was the key phenomenon to realize high concentration of macromolecules inside liposomes (Luisi et al., 2010; Pereira de Souza et al., 2011; Stano et al., 2013; Mavelli and Stano, 2015). Also, a recent study reported that liquid-liquid phase separation of polylactic acids can be a factor for concentrating biomolecules (Jia et al., 2019). Furthermore, it has been reported that hypertonic treatments increase the concentration of macromolecules entrapped in coacervates and liposomes (Fujiwara and Yanagisawa, 2014; Deng et al., 2018). The merit of hypertonic concentration is the simultaneous increase of macromolecular concentration inside the liposomes. The hypertonic concentration can occur in many cases such as the following: evaporation of external solution after liposome formation, immersion of liposomes in hypertonic solution like sea water, and contact with water-absorbing material like hydrophilic crystal or long-chain polyethylene glycols. Therefore, it is plausible that switching of biochemical systems by hypertonic concentration can occur in the natural environment.

These concentration mechanisms can work synergistically. For example, by combining evaporation that could have occurred in the thermal field, overcrowding during vesicle formation, and hypertonic concentration after liposome formation, macromolecular concentration can increase multiplicatively. This multiplicative increase brings an insight to explain the emergence of functional TX-TL by a large jump in the macromolecular concentration. The activation of TX-TL can synthesize membrane proteins that allow flux of small molecules and energy with the outside environment. We showed a proof-of-concept of this scenario (Figure 5). The acquisition of small molecules as the source to rebuild TX-TL machineries is also an important aspect for the emergence of protocells. At this point, switching by hypertonic concentration is beneficial because it induces membrane deformation that increases the surface-area-to-volume ratio and accepts more membrane proteins compared with spherical liposomes.

The system concentration shift is also important for activation of the biochemical systems because response processes to the environmental signal simultaneously increase or decrease subsets of genes. Furthermore, the switching of biochemical systems by the system concentration shift will be utilized as a new tool in bottom-up synthetic biology and biotechnology and can be applied to molecular robots that sense environmental signals to make decision (Hagiya et al., 2014). The system concentration shift may be an overlooked regulator of biochemical systems.

Limitation of this study

The switching property of the TX-TL system appears in limited concentration ranges, and therefore, to use the switching, adequate system concentration should be considered. Although our analysis suggested that other second- or higher-order reactions show similar switching characters against the system concentration shift, we have not confirmed this universality.

STAR★METHODS

Detailed methods are provided in the online version of this paper and include the following:

- KEY RESOURCES TABLE
- RESOURCE AVAILABILITY
  - Lead contact
  - Data and code availability
- MATERIALS AVAILABILITY
- EXPERIMENTAL MODEL AND SUBJECT DETAILS

SUPPLEMENTAL INFORMATION

Supplemental information can be found online at https://doi.org/10.1016/j.isci.2021.102859.

ACKNOWLEDGMENTS

We thank Dr. Satoshi Fujii, Prof. Tomoaki Matsuura (Osaka university), and Prof. Vincent Noireaux (University of Minnesota) for providing the αHL gene. We thank Ms. Rio Iwasaki for English editing of our manuscript. We thank the financial support by JSPS KAKENHI Grant Number JP15H00826 and JP17H05235 to K.F.

AUTHOR CONTRIBUTIONS

K.F. conducted the research. K.F. and S.M.N. conceived the concept. T.A. (mainly) and K.F. (partially) performed all wet experiments. T.A., K.F., M.T., S.M.N., and N.D. analyzed and discussed the data. T.A., K.F., and G.S. performed simulation experiments. K.F. wrote the paper.

DECLARATION OF INTERESTS

The authors declare no competing interests.

Received: March 10, 2021
Revised: July 9, 2021
Accepted: July 12, 2021
Published: August 20, 2021

REFERENCES

Browning, D.F., and Busby, S.J. (2004). The regulation of bacterial transcription initiation. Nat. Rev. Microbiol. *2*, 57–65.

Buddingh, B.C., Elzinga, J., and van Hest, J.C.M. (2020). Intercellular communication between artificial cells by allosteric amplification of a molecular signal. Nat. Commun. *11*, 1652.

Deng, N.N., Vibhute, M.A., Zheng, L., Zhao, H., Yelleswarapu, M., and Huck, W.T.S. (2018). Macromolecularly crowded protocells from reversibly shrinking monodisperse liposomes. J. Am. Chem. Soc. *140*, 7399–7402.

Fujii, S., Matsuura, T., and Yomo, T. (2013). *In vitro* evolution of alpha-hemolysin using a liposome display. Proc. Natl. Acad. Sci. USA *110*, 16796–16801.

Fujiwara, K., Adachi, T., and Doi, N. (2018). Artificial cell fermentation as a platform for highly efficient cascade conversion. ACS Synth. Biol. *7*, 363–370.

Fujiwara, K., and Doi, N. (2016). Biochemical preparation of cell extract for cell-free protein synthesis without physical disruption. PloS one *11*, e0154614.

Fujiwara, K., and Nomura, S.M. (2013). Condensation of an additive-free cell extract to mimic the conditions of live cells. PloS one *8*, e54155.

Fujiwara, K., and Yanagisawa, M. (2014). Generation of giant unilamellar liposomes containing biomacromolecules at physiological intracellular concentrations using hypertonic conditions. ACS Synth. Biol. *3*, 870–874.

Fujiwara, K., Yanagisawa, M., and Nomura, S.M. (2014). Reconstitution of intracellular environments in vitro and in artificial cells. Biophysics (Nagoya-shi) *10*, 43–48.

Hagiya, M., Konagaya, A., Kobayashi, S., Saito, H., and Murata, S. (2014). Molecular robots with sensors and intelligence. Acc. Chem. Res. *47*, 1681–1690.

Hahn, S. (2004). Structure and mechanism of the RNA polymerase II transcription machinery. Nat. Struct. Mol. Biol. *11*, 394–403.

Hilburger, C.E., Jacobs, M.L., Lewis, K.R., Peruzzi, J.A., and Kamat, N.P. (2019). Controlling Secretion in artificial cells with a membrane and gate. ACS Synth. Biol. *8*, 1224–1230.

Jia, T.Z., Chandru, K., Hongo, Y., Afrin, R., Usui, T., Myojo, K., and Cleaves, H.J., 2nd (2019). Membraneless polyester microdroplets as primordial compartments at the origins of life. Proc. Natl. Acad. Sci. USA *116*, 15830–15835.

Kohyama, S., Fujiwara, K., Yoshinaga, N., and Doi, N. (2020). Conformational equilibrium of MinE regulates the allowable concentration ranges of a protein wave for cell division. Nanoscale *12*, 11960–11970.

Kohyama, S., Yoshinaga, N., Yanagisawa, M., Fujiwara, K., and Doi, N. (2019). Cell-sized confinement controls generation and stability of a protein wave for spatiotemporal regulation in cells. eLife *8*, e44591.

Luisi, P.L., Allegretti, M., Pereira de Souza, T., Steiniger, F., Fahr, A., and Stano, P. (2010). Spontaneous protein crowding in liposomes: a new vista for the origin of cellular metabolism. Chembiochem *11*, 1989–1992.

Mansy, S.S., Schrum, J.P., Krishnamurthy, M., Tobe, S., Treco, D.A., and Szostak, J.W. (2008). Template-directed synthesis of a genetic polymer in a model protocell. Nature *454*, 122–125.

Matsuno, R., Nakanishi, K., Ohnishi, M., Hiromi, K., and Kamikubo, T. (1978). Threshold in a single enzyme reaction system. Reaction of maltose catalyzed by saccharifying alpha-amylase from B. subtilis. J. Biochem. *83*, 859–862.

Matsuura, T., Tanimura, N., Hosoda, K., Yomo, T., and Shimizu, Y. (2017). Reaction dynamics analysis of a reconstituted Escherichia coli protein translation system by computational modeling. Proc. Natl. Acad. Sci. U S A *114*, E1336–E1344.

Mavelli, F., Marangoni, R., and Stano, P. (2015). A simple protein synthesis model for the PURE system operation. Bull. Math. Biol. *77*, 1185–1212.

Mavelli, F., and Stano, P. (2015). Experiments on and numerical modeling of the capture and concentration of transcription-translation machinery inside vesicles. Artif. Life *21*, 445–463.

Millard, P., Smallbone, K., and Mendes, P. (2017). Metabolic regulation is sufficient for global and robust coordination of glucose uptake, catabolism, energy production and growth in *Escherichia coli*. Plos Comp. Biol. *13*, e1005396.

Mott, M.L., and Berger, J.M. (2007). DNA replication initiation: mechanisms and regulation in bacteria. Nat. Rev. Microbiol. *5*, 343–354.

Mulkidjanian, A.Y., Bychkov, A.Y., Dibrova, D.V., Galperin, M.Y., and Koonin, E.V. (2012). Origin of first cells at terrestrial, anoxic geothermal fields. Proc. Natl. Acad. Sci. U S A *109*, E821–E830.

Murakami, K.S., and Darst, S.A. (2003). Bacterial RNA polymerases: the wholo story. Curr. Opin. Struct. Biol. *13*, 31–39.

Noireaux, V., and Libchaber, A. (2004). A vesicle bioreactor as a step toward an artificial cell assembly. Proc. Natl. Acad. Sci. U S A *101*, 17669–17674.

Parker, M.W., Botchan, M.R., and Berger, J.M. (2017). Mechanisms and regulation of DNA replication initiation in eukaryotes. Crit. Rev. Biochem. Mol. Biol. *52*, 107–144.

Pereira de Souza, T., Steiniger, F., Stano, P., Fahr, A., and Luisi, P.L. (2011). Spontaneous crowding of ribosomes and proteins inside vesicles: a possible mechanism for the origin of cell metabolism. Chembiochem *12*, 2325–2330.

Ramakrishnan, V. (2002). Ribosome structure and the mechanism of translation. Cell *108*, 557–572.

Shimizu, Y., Inoue, A., Tomari, Y., Suzuki, T., Yokogawa, T., Nishikawa, K., and Ueda, T. (2001). Cell-free translation reconstituted with purified components. Nat. Biotechnol. *19*, 751–755.

Stano, P., D'Aguanno, E., Bolz, J., Fahr, A., and Luisi, P.L. (2013). A remarkable self-organization process as the origin of primitive functional cells. Angew. Chem. Int. Ed. *52*, 13397–13400.

Takahashi, K., Sato, G., Doi, N., and Fujiwara, K. (2021). A relationship between NTP and cell extract concentration for cell-free protein expression. Life *11*, 237.

van den Berg, J., Boersma, A.J., and Poolman, B. (2017). Microorganisms maintain crowding homeostasis. Nat. Rev. Microbiol. *15*, 309–318.

Wu, F., and Tan, C. (2014). The engineering of artificial cellular nanosystems using synthetic biology approaches. Wiley Interdiscip. Rev. Nanomed Nanobiotechnol *6*, 369–383.

Yoshida, A., Kohyama, S., Fujiwara, K., Nishikawa, S., and Doi, N. (2019). Regulation of spatiotemporal patterning in artificial cells by a defined protein expression system. Chem. Sci. *10*, 11064–11072.

Zimmerman, S.B., and Trach, S.O. (1991). Estimation of macromolecule concentrations and excluded volume effects for the cytoplasm of Escherichia coli. J. Mol. Biol. *222*, 599–620.

STAR★METHODS

KEY RESOURCES TABLE

REAGENT or RESOURCE	SOURCE	IDENTIFIER
Bacterial and virus strains		
Escherichia coli BL21-CodonPlus(DE3)-RIPL	Agilent Technologies,	Cat# 230280
Chemicals, peptides, and recombinant proteins		
Folinic acid	Tokyo Chemical Industry	Cat# C2235
Ultrapure water	Thermo Fisher Scientific	Cat# 10977023
Potassium glutamate	Sigma-Aldrich	Cat# G1501-1KG
Magnesium glutamate	Sigma-Aldrich	Cat# 49605-250G
Magnesium acetate	Nacalai tesque	Cat# 208-21
tRNA	Roche	Cat# 10109541001
Creatine kinase	Roche	Cat# 10127566001
ATP	Wako Chemical	Cat# 014-16913
GTP	Wako Chemical	Cat# 073-03113
CTP	Tokyo Chemical Industry	Discontinued
UTP	Affymetrix	Discontinued
IPTG	Nacalai tesque	Cat# 19742-94
Tris(hydroxymethyl)aminomethane	Nacalai tesque	Cat# 35434-05
NaCl	Nacalai tesque	Cat# 31320-05
Imidazole	Nacalai tesque	Cat# 19004-35
HEPES	Nacalai tesque	Cat# 17546-05
HCl	Nacalai tesque	Cat# 18321-05
KOH	Nacalai tesque	Cat# 28616-45
Sucrose	Nacalai tesque	Cat# 30404-45
20 Amino acids (5 mM each)	This study	see Table S1
Spermidine	Nacalai tesque	Cat# 32108-91
Creatine phosphate	Wako Chemical	Cat# 030-04584
Chloroform	Nacalai tesque	Cat# 08402-55
1-Palmitoyl-2-Oleoylphosphatidylcholine (POPC)	Avanti	Cat# 850457C
Biotinyl-Cap-PE	Avanti	Cat# 870273C
Rhodamine-PE	Avanti	Cat# 810150C
Calcein-AM	Nacalai tesque	Cat# 06735-81
NuSieve GTG Agarose	Lonza	Cat# 50081
Lysozyme	Nacalai tesque	Cat# 19499-04
NdeI	New England Biolabs	Cat# R0111S
XhoI	New England Biolabs	Cat# R0146S
PrimeSTAR MAX DNA polymerase	TAKARA	Cat# R045B
sfGFP	This study	N/A
TagBFP2	This study	N/A
mCherry	This study	N/A
Ampicillin	Nacalai tesque	Cat# 02739-32
Kanamycin	Nacalai tesque	Cat# 19860-44

(*Continued on next page*)

Continued

REAGENT or RESOURCE	SOURCE	IDENTIFIER
Critical commercial assays		
HisTrap HP	GE Healthcare	Cat# 17524701
Amicon-Ultra 15 filter 10k	MilliporeMerck	Cat# UFC901096
BCA Assay kit	Thermo Fisher Scientific	Cat# 23225
PUREfrex1.0	Genefrontier	Cat# PF001-0.25-5
Oligonucleotides		
Primers	This study	see Table S2
Recombinant DNA		
pET15-sfGFP	Fujiwara and Nomura, 2013	N/A
pET29-sfGFP	Fujiwara and Doi, 2016	N/A
pET15-TagBFP2	This study	N/A
pET29-mCherry-His	This study	N/A
pET29-αHL	This study	N/A
Software and algorithms		
PURE system simulator	Matsuura et al., 2017	https://sites.google.com/view/puresimulator

RESOURCE AVAILABILITY

Lead contact

Further information and requests for resources and reagents should be directed to and will be fulfilled by the lead contact, Kei Fujiwara (fujiwara@bio.keio.ac.jp).

Data and code availability

This paper does not report original code. For questions regarding this study, please contact the corresponding author. All software used in this study are available commercially or from the developer's website.

MATERIALS AVAILABILITY

Plasmids constructed in this study are available from the corresponding author on request.

EXPERIMENTAL MODEL AND SUBJECT DETAILS

A commercial strain, *Escherichia coli* BL21-CodonPlus(DE3)-RIPL (*E. coli B F*$^{-}$ *ompT hsdS*($r_B^- m_B^-$) *dcm*$^+$ *Tet*^{r} *gal λ*(DE3) *endA Hte [argU proL Cam*^{r}*] [argU ileY leuW Strep/Spec*^{r}*]*), which was purchased from Agilent Technologies, was used to express proteins purified in this study and as a source of cell extract.

METHOD DETAILS

Chemicals

Folinic acid (FD) and CTP were purchased from Tokyo Chemical Industry (Tokyo, Japan). Potassium glutamate (GluK) and magnesium glutamate (GluMg) was purchased from Sigma-Aldrich (St. Louis, MO, USA). tRNA and creatine kinase (CK) were purchased from Roche (Basel, Switzerland). ATP and GTP were purchased from Wako Chemical (Osaka, Japan). UTP was purchased from Affymetrix (Santa Clara, CA, USA). Other chemicals were purchased from Nacalai tesque (Kyoto, Japan). 1x NTP indicates a mixture of 2.0 mM ATP, 2.0 mM GTP, 1.3 mM UTP, and 1.3 mM CTP. Ultrapure water was purchased from Thermo Fisher Scientific (Waltham,MA. Catalog code: 10977023).

Plasmid construction

pET15-sfGFP, pET29-sfGFP were prepared in previous studies (Fujiwara and Nomura, 2013; Fujiwara and Doi, 2016). pET15-TagBFP2, pET29-mCherry-His, pET29-αHL were constructed in this study. pET15-TagBFP2 was constructed by ligation of NdeI/XhoI-digested fragments of pET15b vector (Merck Millipore,

Billerica, MA, USA) and a synthesized gene of TagBFP2 (Thermo Fisher Scientific). pET29-mCherry-His was constructed by removing *minE* gene from pET29-MinE-mCherry-His (Kohyama et al., 2019) by PCR and a primer set (pET29mCherryFw/pET29u). pET29-αHL was constructed by fusing pET29 vector amplified by a primer set (pET29d/pET29u) with C-terminal histidine-tagged αHL gene (Fujii et al., 2013) prepared by PCR. PCR fragments were converted to plasmids by SLIC method. To attach DNA histidine-tag to αHL gene, two times PCR was performed using primer sets (aHLfw/aHLrv1 for 1st PCR, aHLfw/aHLrv1 for 2nd PCR). PrimeSTAR MAX DNA polymerase was used for all PCR, and all DNA sequences were verified by Sanger DNA sequencing. Primer sequences are shown in Table S2.

Protein purification

sfGFP, TagBFP2, and mCherry were purified in our laboratory. *E. coli* BL21-CodonPlus(DE3)-RIPL (Agilent Technologies, Santa Clara, CA, USA) harboring pET15-sfGFP, pET15-TagBFP2, or pET29-mCherry-His were cultivated in LB medium with ampicillin or kanamycin, and target proteins were overexpressed by 0.1 mM isopropyl b-D-1-thiogalactopyranoside (IPTG) addition at OD_{600} = 0.4. Then, cells were further cultivated overnight at 37°C (sfGFP) or 18°C (TagBFP2 and mCherry). The cells were collected by centrifugation, and disrupted by sonication after dissolving with NiA buffer [50 mM Tris-HCl (pH8.0), 500 mM NaCl, and 40 mM imidazole]. The target proteins were purified with AKTA start using HisTrap column (GE Healthcare, Chicago, IL, USA). The proteins were eluted by NiB buffer [50 mM Tris-HCl (pH8.0), 500 mM NaCl, and 400 mM imidazole]. Buffer was exchanged with 20 mM HepesKOH by using Amicon-Ultra 15 filter (10 kDa, MilliporeMerck). Proteins were stored at -30°C.

Preparation of S30 extract for TX-TL reactions

S30 extract was prepared according to the previous report (Fujiwara and Doi, 2016) because the method does not require any special apparatus. The detail of the method is as follows. *E. coli* BL21-CodonPlus(DE3)-RIPL was pre-cultured in LB medium without antibiotics, inoculated into 1 L of LB medium (0.5% final), and cultured at 37°C for 1 h. Then, IPTG was added at 0.1 mM final for T7RNA polymerase induction, and the culture was further cultivated at 37°C to reach OD_{600} =1.2.

The culture was harvested by 10000 x *g* centrifugation at 4°C for 3 min. The collected cells were dissolved with 10 mL of 400 mM sucrose. Cells were pelleted again by centrifugation, and were dissolved by 10 mL of 400 mM sucrose. Then, 200 μL of 20 mg/mL lysozyme (Nacalai tesque) was added. After incubating on ice for 1 h, cells were collected by centrifugation in the same manner as above. Then, cells were washed with 20 mL of 400 mM sucrose twice. Collected cells were suspended with chilled 1.5 mL S30A buffer [10 mM Tris-HCl (pH 7.6), 60 mM GluK, 10 mM magnesium acetate] per 1 g of cell mass. Then, the suspension was dispensed in 1 mL portions into a 1.7 mL tube. Tubes were frozen in liquid nitrogen for 15 min, and then, thawed in ice water for 1 h. The freeze-thawed cells were centrifuged at 30,000×*g* for 1 h at 4°C. The supernatant after the centrifugation was washed and concentrated by using S30B buffer [10 mM Tris-HCl (pH 7.6), 60 mM GluK, 14 mM magnesium acetate] and Amicon-Ultra 10 k filter. Protein concentrations in the supernatant were quantified by BCA Assay kit (Thermo Fisher Scientific). For dilution of TX-TL system, ultrapure water was used. To concentrate S30 in bulk, water was carefully evaporated under argon gas flow.

TX-TL reactions in tubes

Reaction mix [4.76 x NTPs, 2.86 mM each amino acids, 4.76 mM spermidine, 0.943 mg/mL tRNA, 476 mM GluK, 71.4 mM GluMg, 238 mM HEPES-KOH (pH 7.6), 0.323 mM FD, 381 mM creatine phosphate (CP), 4.76 mM IPTG] was prepared and stored at -30°C. Reaction solution [various concentrations of S30, 20 ng template DNA, 2.1 μL of reaction mix, 0.3 μL of 10 mg/mL CK, and filled up to 10 μL with ultrapure water] was prepared. As the DNA template, pET29-sfGFP was used. The normal S30 concentration was set at 10 mg/mL. To prepare the diluted TX-TL system, the reaction solution or S30 was diluted by ultrapure water. In PURE system, PURExpress1.0 (Genefrontier, Chiba, Japan) with 20 ng template DNA was used. All TX-TL reactions were performed at 37°C for 3 h or 15 h if indicated. Expression levels of sfGFP were quantified by fluorescence levels of the corresponding band after non-boil SDS-PAGE using a fluorescence imager, and ImageJ software.

Simulation of TX-TL system

Simulations were performed according to the model established in a previous report (Mavelli et al., 2015). The detail of the model is as follows. All reaction formula, parameters, and initial concentrations were

shown in Figure S5. Concentration used in the previous report was set as 1 of the system concentration. Levels of protein expression after 3 h reaction were calculated. The time evolution by the differential equations was analyzed by the difference method. Simulation was executed with Perl script.

For the simulation using a detailed translation model, PURE system simulator (Matsuura et al., 2017) was downloaded from the developers website, and was executed in MATLAB (Mathworks, Natick, MA, USA) as we performed in a previous study(Takahashi et al., 2021). In this model, all biochemical reactions in TX-TL reactions are implemented and are analyzed by ordinary differential equations (ODE). All simulations were performed for 10,000-sec reaction using ODE15s. The concentration of elements in PURE system was initial sets of the simulator except mRNA concentration was tripled to make the concentration of mRNA correspond to the simple model.

Liposome preparation

Liposomes were prepared by the droplet-transfer method according to our previous report (Fujiwara and Yanagisawa, 2014) because of its easiness of entrapping molecules. The detail of the method is as follows. To prepare lipid solution, 40 μL of 25 mg/mL 1-Palmitoyl-2-Oleoylphosphatidylcholine (POPC, Avanti, Alabaster, AL, USA) dissolved in $CHCl_3$ was added to glass tubes. In the case of GFP concentration and fixation of liposomes using a streptavidin-coated glass (Video S1), 2.5 μL of 0.1mg/mL Rhodamine-PE (Avanti) and 0.1 mg/mL Biotinyl-Cap-PE (Avanti) were added to the lipid solution, respectively. After evaporating the solution under argon gas, 500 μL of mineral oil was added to the lipid-dried tube and sonicated for 90 min in a hot water bath at 60°C. After the sonication, 1 minute vortex was performed to mix the solution.

In a fresh 1.7 mL tube, 100 μL of external solution of liposomes (solutions of S30 reaction mixture without S30 or PUREfrex solution without enzymes) and 50 μL of lipid solution were placed in this order. In another tube, 4 μL of the solution to be entrapped in liposomes (hereafter called as the inner solution) was added to 50 μL of the lipid solution, and then, emulsions were prepared by tapping. The prepared emulsions were carefully placed above the external solution. Liposomes were formed by centrifugation at 10,000×*g* for 30 min at 4°C, and were collected by removing the oil layer using pipetts. Then, the external solution containing liposomes was collected as a liposome solution and stored in another fresh tube. All liposomes were prepared immediately before experiments.

Hypertonic treatment of liposomes with sfGFP protein

To analyze the relation between sfGFP concentration and fluorescence intensities, liposomes were prepared using sfGFPmix (various concentrations of sfGFP, 5 mg/mL BSA, and 10 mM sucrose) as the inner solution, and 30 mM glucose as the external solution. To obtain the standard curve, 100 μg/mL, 200 μg/mL, 400 μg/mL, 800 μg/mL, 1000 μg/mL, 2000 μg/mL, 3000 μg/mL, and 4000 μg/mL sfGFP were used. After incubation of the liposome solution on cover glasses at room temperature for 1 h, fluorescent images were acquired with a confocal microscope. By using ImageJ on the images, a calibration curve of sfGFP concentration against fluorescence intensity was obtained.

To test the hypertonic concentration of sfGFP within liposomes, the liposomes containing 100 μg/mL sfGFP were examined with hypertonic treatment by mixing with the same volume of 90-870 mM sucrose. For applying 20 times and 30 times higher osmolytes, 16 μL of 742.5 mM sucrose was added to 4 μL of the liposome solution, and 15 μL of 1190 mM sucrose was added to 5 μL of the liposome solution, respectively.

Hypertonic treatment of liposomes with diluted TX-TL systems

A reaction solution (2.2 μL of 45 mg/mL S30, 20 ng template DNA, 2.1 μL of reaction mix, 0.3 μL of 10 mg/mL CK, each fluorescent protein (1.5 mg/mL TagBFP2 or mCherry) to indicate liposomes, and filled up to 10 μL by ultrapure) was prepared as the internal solution of the liposome. As the DNA templates, pET15-MetK, pET29-sfGFP, and pET29-aHL were used. For α-HL expression, 100 μM calcein was added to the inner solution. As the external solution, 32 μL of a mixture of the reaction mix, 23 μL of S30B buffer, and 45 μL of ultrapure water was prepared. To prepare the 1/5-fold diluted TX-TL solution, 2 μL of the reaction solution was diluted with 8 μL of ultrapure water. To prepare liposomes with the 1/5-fold diluted TX-TL system, the external solution was similarly diluted with ultrapure water. A 1620 mM sucrose solution or 2x external solution (32 μL of reaction mix, 2.3 μL of 10×S30 B buffer, 15.7 μL of ultra pure water) was prepared as a liposome concentrating agent. In the case of PURE system, the internal solution was the PUREfrex 1.0 with 20 ng

template DNA or its 1/5 diluent by Ultrapure water, and PUREfrex Sol I (small molecule mixture supplied) diluted with the same volume of Ultrapure water was used as the osmolytes.

For hypertonic treatments, 3 μL of osmolytes were added to 3 μL of the liposome solution prior to being spotted on a cover glass. To prevent evaporation, the cover glass with liposomes were sealed with silicone rubber and another cover glass. After 3 h incubation at 37°C, fluorescent images of liposomes were captured with a fluorescence microscope (Zeiss AxioVert observer Z1) or a confocal microscope (FV1000). The fluorescence intensity of the liposome was quantified by ImageJ. Diameters of liposomes were estimated from circular surface area obtained from binary images of fluorescence of indicator proteins (sfGFP) detected by Otsu method packaged in ImageJ and dividing surface area ($2\pi \times$ diameter) by 2π.

Fluorescence imaging of liposomes fixed in agarose gels

To fix liposomes at the same microscopic field, we used agarose fixation method because its easiness. For agarose fixation of liposomes, NuSieve GTG Agarose (Lonza, Basel, Switzerland) dissolved in ultrapure water was mixed with the same volume of the liposome solution to prepare 1% agarose solution. Then, 5 μL of the solution were dropped onto a cover glass, and incubated for 5 min at 37°C, and for 15 min at 4°C, to gelate agarose. To observe the osmolyte-induced TX-TL activation, time-lapse images were obtained after addition of the osmolyte (S30 reaction mixture). Fluorescent images were periodically obtained using fluorescent microscope and Micromanager software. Fluorescence intensities of each liposome on time were quantified with ImageJ.

QUANTIFICATION AND STATISTICAL ANALYSIS

In this study, no statistical analysis such as t-test were performed. Exact value of n (liposomes) and precision measures are shown in figure legends.